IOSR Journal Of Applied Physics (IOSR-JAP)
e-ISSN: 2278-4861.Volume 18, Issue 1 Ser. 1 (Jan – Feb 2026), PP 52-59
www.Iosrjournals.Org

Computational Analysis And An Excited-State Intramolecular Hydrogen Atom Transfer Investigation On Ortho-Vanillin: A Micro-Solvation Study

Dr. Jagadeesha. K, M. Premsingh, Chandraiah. T, Dr. Srinivas. P
(Department Of Physics, Maharani Science College For Women (Autonomous), Mysore-570005, Indi)
(Department Of Computer Science, Government College (Autonomous), Mandya-571401, India)
(Department Of Computer Science, Yuvaraja College, Mysore-570005, India)
(Department Of Physics, Maharani Science College For Women (Autonomous), Mysore-570005, India)

Abstract:
In this work, we study the structural properties of Ortho-Vanillin (OVA) and micro solvated molecule [OVA + $(H_2O)_3$ -OVAH] as a theoretical investigation. An intra-molecular hydrogen bond exists between hydrogen of hydroxyl group and oxygen of benzaldehyde group in both OVA and OVAH molecules. The ground (S_0) / excited (S_1) electronic properties of both molecules were computed using density functional theory (DFT) / time-dependent density functional theory (TDDFT) by employing B3LYP/cc-pvDZ basis set by using GAMESS program. The stability of the molecules has been investigated using the natural bond orbital (NBO) analysis. The highest occupied molecular orbital (HOMO) energies, the lowest unoccupied molecular orbital (LUMO) energies have been calculated and the electronic properties like energy gap, ionization potentials, electron affinities, chemical potential, chemical hardness, softness, electrophilic index which are depends on HOMO-LUMO energies were determined. The molecular electrostatic potential (MEP) of both molecules was computed in order to predict the relative reactivity of nucleophilic and electrophilic attack. And also, both OVA and OVAH molecules exhibits Excited-State Intramolecular Hydrogen atom transfer (ESIHT) mechanism.

Key Word: *Density functional theory, Time-dependent density functional theory, Polarizable continuum model, Natural bond orbital. etc.,*

Date of Submission: 17-02-2026 Date of Acceptance: 27-02-2026

I. Introduction

A comprehensive investigation of hydrogen bonds is significantly crucial for grasping the photophysical properties of various organic compounds with electron donor and acceptor mechanisms at ground and excited states [1,2,3,4]. The EFP approach provides a polarizable QM-based force field for characterizing intermolecular interactions. To explore the micro solvation effect on biological or organic molecules, the EFP1/DFT approach was explicitly customized for solvation and interfaced with the polarizable continuum model (PCM)[5,6]. Moreover, the EFP1/TDDFT approach has been promoted for describing the electronically excited states of molecules that have been solvated [5,7,8,9]. To understand the electrical, molecular, structural, and photophysical properties of organic and biological molecules, time-dependent density functional theory (TDDFT) simulations are performed in excited states. In the excited state, hydrogen transfer and molecular structural refashioning occur inside the molecule.

The ESIPT/ESIHT process in certain chemical and biological molecules is demonstrated by the redesign of hydrogen bond anatomy brought about by the micro solvation effect[10]. The photophysical properties of biologically active compounds are linked to their intra-molecular charge transfer (ICT) and ESIPT/ESIHT characteristics[11].

OVA is trisubstituted benzene with -CHO, -OH and -OCH3 groups across first, second and third positions having intra-molecular hydrogen bond O9-H10·····O11=C7 across hydroxyl and benzaldehyde groups. *OVA* mainly exists in vanillin and other plant extracts, such as *Pinus koraiensis* fruit, Helichrysum genus, oak (*Quercus*)[12,13,14,15]. *OVA* has already been widely applied in food, beverage, pharmacy, and cosmetics[16]. Several benzaldehydes are identified having potent antifungal activity against strains of Aspergillus fumigatus, A. flavus, A. terreus and Penicillium expansum, fungi that are causative agents of human invasive aspergillosis and/or are mycotoxigenic. OVA showed the highest antifungal activity[17]. *OVA* was tested for its cytotoxic and nuclear factor kappa-B (NF-κB) inhibitory activities in cultured A375 human melanoma cells and also *OVA* deserves further evaluation as potential anticancer drugs[18]. *OVA* is an isomer of the well-known food supplement vanillin and was studied in different malignancies including colon, ovarian and lung cancer and melanoma [19,20,21]. *OVA* have phenolic –OH, which is responsible for the free radical scavenging activity and it is a more effective quencher of DPPH (1,1-diphenyl-2 picrylhydrazyl) radical because it donated an electron to

DPPH more easily[21]. *OVA* is the main metabolite and it has documented anti-inflammatory and antioxidative properties[22].

II. Computational Calculations

The OVA and OVAH molecules were modelled using Avogadro [23] molecular modelling package and optimized with MMFF94s[24] force field. Using the generated coordinates of the molecules from the Avogadro package, all required calculations have been performed using the NBO.6[25] unified GAMESS[26,27] software suite. The ground and first excited state optimisation of OVA and OVAH molecules were carried out at the level of DFT [28,29,30,31,32] / TDDFT [33,34] with B3LYP[35,36] hybrid functional by employing cc-pVDZ basis set[37]. Based on optimized ground state geometry, absorption energies were computed using TDDFT / cc-pVDZ / B3LYP / PCM / EFP1[38,39,40] method. Natural charges were calculated both in ground and first excited states by using NBO.6 method. Molecular orbitals, Molecular electrostatic potential maps were plotted using wxMacMolPlt [41] by using log file which is obtained from GAMESS software.

III. Results And Discussion

Molecular geometrical parameters at S_0 and S_1 states

The optimized structural parameters like bond lengths and bond angles of OVA and OVAH molecules at ground (S0) and excited state (S1) were computed from DFT/TDDFT/B3LYP/ cc-pVDZ and are listed in **Table-1,** in accordance with the atom numbering scheme given in **Figure:1-2**. In OVA molecule, intra-molecular HB O9-H10·····O11=C7 (1.698 A^0) in S0 state alters as O11-H10·····O9=C5 (1.519A^0) in the S1 state. In OVAH molecule, intra-molecular HB O9-H10·····O11=C7 (2.134 A^0) in S0 state alters as O11-H10···· ·O9=C5 (1.822A^0) in the S1 state. When OVA excited to S1 state, the bond lengths C2-C3/ C4-C5/ C5=C6/ O8-C16/ C7=O11/ O9-H10/ C6-C1/ C3-H14 increased by 0.044/ 0.014/0.037/ 0.009/0.089/0.524/0.034/0.002 A^0, whereas bond lengths C1=C2/ C3=C4/ C6-O8/ C5-O9/ C7-H12/ C16-H17/ C16-H18/ C16-H19/C2-H13 decreased by 0.03/0.017/ 0.023/0.057/0.022/0.001/0.003/0.002/0.001 A^0. The bond angles between the respective atoms decrease / increase in the range (0.3-6.5^0) / (0.2-3.2^0).

The optimized structural parameters of OVAH molecule are changed due to the effect of micro solvation. The bond lengths C2-C3 / C5=C6 / C6-O8/ O8-C16/ C7-H12 increased by 0.001 / 0.002 / 0.011 / 0.002 / 0.005 A^0, whereas bond lengths C1=C2/ C4-C5/ C5-O9/ C7=O11/ O9-H10/ C6-C1 decreased by 0.002 / 0.001 / 0.005 / 0.013 / 0.009 / 0.003 A^0. The bond lengths C16-H17, C16-H18, C16-H19, C1-H15, C2-H13 and C3-H14 are unaltered. The bond angles between the respective atoms decrease / increase in the range (0.3-3.2^0) / (0.2-10.9^0). When OVAH excited to S1 State, the bond lengths C2-C3/C4-C5/C5=C6/O8-C16C7=O11/O9-H10/C6-C1/C3-H14 increased by 0.045/0.015/0.037/0.006/0.098/0.836/0.035/0.002A^0, whereas bond lengths C1=C2/C3=C4/C6-O8/C5-O9/C7-H12/C16-H17/C16-H18/C16-H19/C2-H13 decreased by 0.028/0.016/0.03/ 0.06/0.0280.001/0.003/0.002/0.001 A^0 and bond length C1-H15 remains unaltered. The bond angles between the respective atoms decrease / increase in the range (0.1-5.8^0) / (0.7-15.6^0).

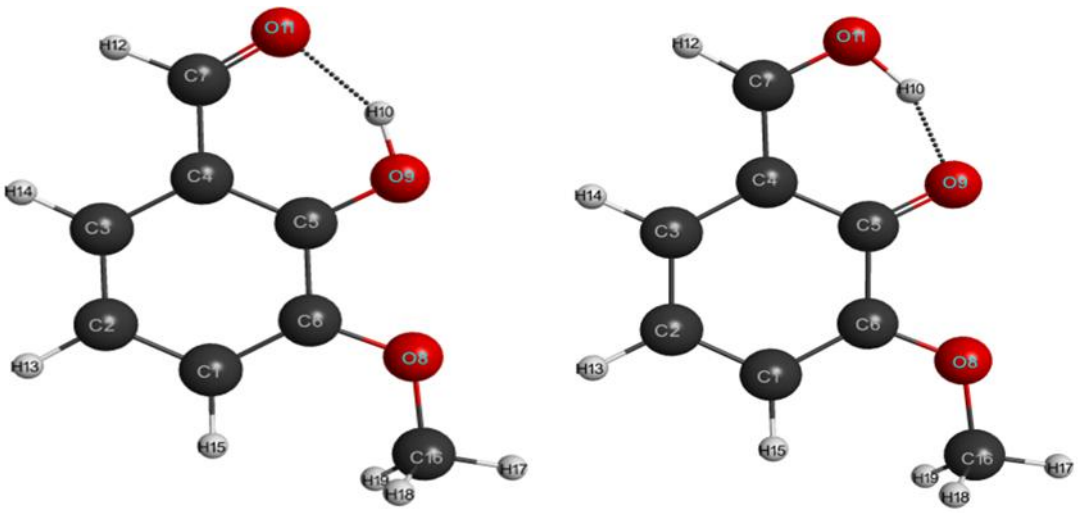

a) **(b)**

Figure-1: Optimized equilibrium molecular structures of OVA molecule at (a) S_0 (b) S_1 states.

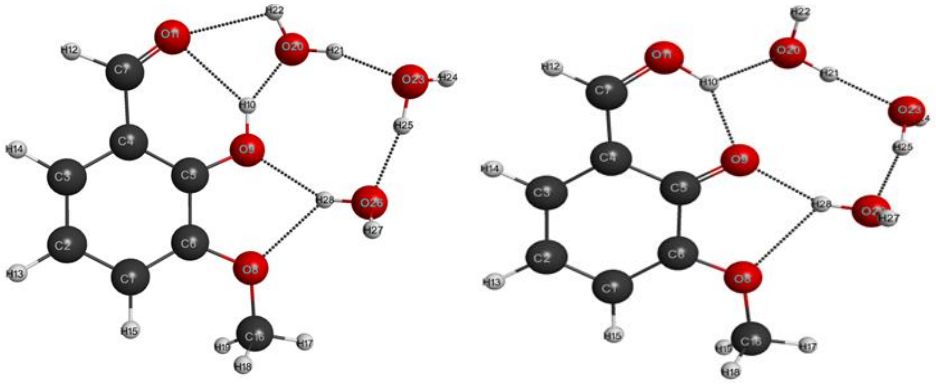

a) **(b)**

Figure-2 : Optimized equilibrium molecular structures of OVAH molecule at (a) S_0 (b) S1 states.

Bond angles and Bond lengths	OVA-S0	OVA-S1	OVAH -S0	OVAH-S1
C_1-C_7=C_3	119.9	119.0	119.6	118.9
C_7-C_3=C_4	119.9	122.9	121.0	123.3
C_3=C_4-C_5	120.5	120.2	119.8	119.9
C_4-C_5=C_6	119.1	116.0	118.4	115.6
C_5=C_6-C_1	119.3	122.5	120.7	123.3
C_6-C_1=C_7	121.3	119.5	120.5	118.9
C_1-C_6-O_8	125.9	123.5	125.5	123.9
C_6-O_8-C_{16}	118.0	120.5	118.2	121.0
O_8-C_6-C_5	114.8	114.0	113.8	112.8
C_6-C_5-O_9	118.5	121.4	115.3	121.1
C_5-O_9-H_{10}	105.9	99.4	116.8	101.2
C_4-C_5-O_9	122.4	122.6	126.3	123.2
C_5-C_4-C_7	118.9	118.5	122.0	120.2
C_4-C_7=O_{11}	124.5	120.5	126.0	123.9
O_{11}-C_7-H_{12}	119.5	116.7	120.3	114.9
C_7-C_4=C_3	120.6	121.3	118.1	119.9
C_1=C_7	1.412	1.382	1.410	1.382
C_7-C_3	1.381	1.425	1.382	1.427
C_3=C_4	1.416	1.399	1.416	1.400
C_4-C_5	1.416	1.430	1.415	1.430
C_5=C_6	1.423	1.460	1.425	1.462
C_6-O_8	1.359	1.336	1.370	1.340
O_8-C_{16}	1.418	1.427	1.420	1.426
C_5-O_9	1.336	1.279	1.331	1.271
C_7=0_{11}	1.234	1.323	1.221	1.319
O_9-H_{10}	0.995	1.519	0.986	1.822
C_6-C_1	1.393	1.427	1.390	1.425
C_7-H_{12}	1.116	1.094	1.121	1.093
C_{16}-H_{17}	1.098	1.097	1.098	1.097
C_{16}-H_{18}	1.106	1.103	1.106	1.103
C_{16}-H_{19}	1.105	1.103	1.105	1.103
C_1-H_{15}	1.090	1.090	1.090	1.090
C_2-H_{13}	1.091	1.090	1.091	1.090
C_3-H_{14}	1.093	1.095	1.093	1.095

Table-1: Selected bond angles – A (°) and bond lengths-r (A^0) of OVA and OVAH molecules at S_0 and S_1 states.

Natural bond orbital (NBO) analysis

Charge transfer interactions between OVA and OVAH molecules can be understood in a detailed manner using natural bond orbital (NBO) analysis. Intramolecular charge transfer takes place to provide stability to a structure in a given environment. Natural charge analysis for both OVA and OVAH molecules at ground and excited states using DFT / TDDFT / B3LYP / cc-pVDZ with NBO 6.0 package which incorporate with GAMESS-US software and are tabulated in **Table-2.**

Atom number	OVA-SO	OVA-S1	OVAH-SO	OVAH-S1
C_1	-0.2796	-0.27752	-0.28230	-0.27655
C_2	-0.2467	-0.25681	-0.24874	-0.25823
C_3	-0.20306	-0.05493	-0.20288	-0.05549
C_4	-0.24858	-0.28404	-0.24098	-0.27278
C_5	-0.37534	0.35875	0.36901	0.35737
C_6	0.27983	0.35305	0.26908	0.33981
C_7	0.40166	0.18996	0.40118	0.19815
C_8	-0.27162	-0.44729	-0.55306	-0.4713
O_9	-0.52144	-0.68074	-0.72967	-0.72468
O_{10}	-0.66460	0.50728	0.62418	0.57106
O_{11}	-0.58313	-0.64904	-0.57014	-0.63343
H_{19}	0.50626	0.18571	0.13224	0.18231
H_{12}	0.15268	0.23707	0.23326	0.23625
H_{13}	0.23402	0.23010	0.23081	0.22918
H_{14}	0.23155	0.23573	0.23532	0.23504
H_{15}	0.23669	-0.27922	-0.27160	-0.27722
H_{17}	0.22100	0.22879	0.22090	0.23232
H_{18}	0.18985	0.20078	0.18880	0.19892
H_{16}	0.18996	0.20237	0.19458	0.20126

Table-2: Natural charges on different atoms of OVA / OVAH molecules at S_0 and S_1 states.

The natural charges on atoms of OVA and OVAH molecules alters due to the effect of micro solvation. Natural charges on C1/C2/O8/O9/H10/H19 increased by -0.0027e/ -0.0019e / -0.0317e / -0.0651e / 0.1179e / 0.0046e. whereas natural charges on C3 / C4 /C5 /C6 /C7 /O11/ H12 /H13 / H14/ H15/H17/H18 decreased by -0.0002e / -0.0076e / 0.0063e / 0.0107e / 0.0005e /-0.013e / 0.0205e / 0.0007e /0.008e /0.0014e /0.0001e /0.0011e. Due to photo-excitation, the natural charges on atoms of OVA molecule changes. The charges on C2/C4/C6/O9//H10/O11/H12/H13/C16/H17/H18/H19 increased by -0.01e/-0.0354e /0.0733e/ 0.0161e /0.001e /-0.0659e /0.033e /0.0031e /-0.0076e / 0.0078e /0.0109e /0.0124e. whereas charges on C1/ C3/ C5/ C7/ O8/ H14/H15 decreased by -0.0021e /-0.1482e /0.0165e /0.2117e /-0.0741e /0.0015e / 0.001e. Due to photo-excitation, the natural charges on atoms of OVAH molecule also changes. The charges on C2 /C4 /C6 /O11 /H12 /H13 /H17 /H18 /H19 increased by -0.0095e/-0.0418e/-0.0707e/-0.0633e /0.0501e / 0.003e/ 0.0114e/ 0.0101e/0.0067e. whereas charges on C1 / C3 /C5 /C7 /O8 /O9 /H10 /H14 /H15 decreased by -0.0037e/ -0.1474e /0.0116e /0.203e /-0.0818e /-0.005e /0.0531e / 0.0016e /0.0003e.

Molecular orbitals

The molecule's ability to donate and receive electrons is characterized by its HOMO and LUMO energies. Molecular orbitals are important for electrical and optical characteristics, luminescence, photochemical reactions, UV-VIS, quantum chemistry, pharmacological investigations, and understanding biological mechanisms. Furthermore, MOs aid in anticipating the most reactive site of the given molecule. The prominent molecular orbitals called LUMO and HOMO of OVA and OVAH molecules are computed by DFT / TDDFT / B3LYP / cc-pVDZ methods and are illustrated in **Figures 3-4.**

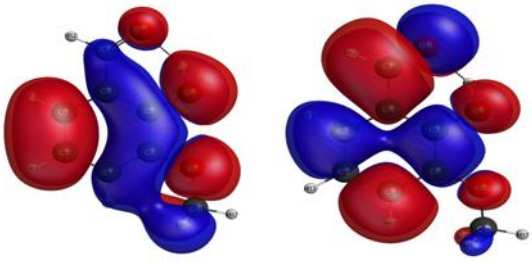

HOMO(-5.8232eV) LUMO(-1.7959eV)
Figure-3: The molecular orbitals of OVA molecule.

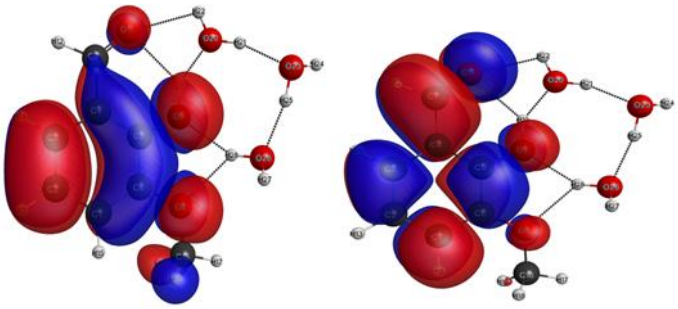

HOMO(-5.7688eV) LUMO(-1.4966eV)
Figure-4: The molecular orbitals of OVAH molecule.

The chemical reactivity parameters of OVA and OVAH molecules such as chemical potential (μ), electronegativity(χ), chemical hardness (η), electrophilicity index (ω) and softness (S) were also carried out with the help of energy of HOMO and LUMO orbitals and tabulated in **Table-3.**

Chemical reactivity parameters	OVA	OVAH
E_{homo}(eV)	-5.8232	-5.7688
E_{Lumo}(eV)	-1.7959	-1.4966
Ionisation Potential (IP)	5.8232	5.7688
Electron affinity (EA)	1.7959	1.4966
ΔE_{gap}(eV) = $E_H - E_L$	**4.0273**	**4.2722**
Chemial potential(μ)= - (IP+EA)/2	-3.8095	-3.6327
Eectronegetivity(χ) = - μ	3.8095	3.6327
Hardness(η) =(IP-EA)/2	2.0136	2.1361
Electrophilic index(ω) = $\mu^2/2\eta$	3.6035	3.0889
Softness(S)=1/2η	0.2483	0.2340

Table-3: Chemical reactivity parameters of OVA and OVAH molecules

It is observed that, the OVAH molecule have the highest energy gap 4.2722 eV compare to OVA molecule which has energy gap of 4.0273eV. which means that increase of the HOMO-LUMO energy gap in OVAH molecule decreases reactivity of the compound that leads to increase in the stability of the molecule. And also lower the ionization potential of OVAH molecule, easier is to remove an electron from a molecule. So, OVAH molecule is less polarizable and is associated with a low chemical reactivity, high kinetic stability and is also termed as hard molecule. And also, OVAH has lowest value of the Ionisation potential (IA =5.7688 eV), so that it will be the better electron acceptor. The Chemical hardness value of OVAH molecule is 2.1361eV is greater as compare with OVA molecule which is having 2.0136eV Thus, OVAH molecule is found to be more reactive than OVA molecule. The softness value of OVAH molecule is 0.2340eV is lesser as compare with OVA molecule which is having 0.2483eV. Thus, OVAH molecule is found to be more reactive than OVA molecule.

Molecular electrostatic potential (MEP)

To study the reactive behaviour of OVA and OVAH molecules, MEP is computed at its outer surface both at ground and excited states by DFT / TDDFT / B3LYP / cc-pVDZ methods**.** MEP of OVA and OVAH molecules can be used for better interpretation of its interactions with other molecules, particularly for the prediction of protonation sites. The different colours on the surface which represent various values of the electrostatic potential. Red, green and blue colours indicate the regions of most electronegative(electron-rich), neutral and most positive electrostatic potential(electron-insufficient) respectively. As can be seen from the MEP, it was clear that best area (blue) is restricted on the H molecules, which can show a conceivable site for nucleophilic attack. In the intermediary, electrostatic potential areas (red) were basically limited over the O9, O11 and O8 atoms, demonstrating the most good site for electrophilic attack. It is clear from figures (4) likewise the zero electrostatic surface potential (green hues) in the focal point of OVA and OVAH molecules. It is observed that the total charge on aldehyde / Hydroxy / methoxy groups of "OVA" and "OVAH" molecules are "0.1527e / -0.1583e / -0.1922e" and "0.2333e / -0.1055e / -0.2204e" at S0 state, and that in S1 state are "0.2371e / -0.1735e / -0.0945e" and 0.2363e / -0.1536e / -0.116e. The net charge on benzene ring in OVA and OVAH molecules are "-1.0735 e, -0.1615e" and "-0.3368e, -0.1779e" in "S0, S1" states. MEP of OVA and OVAH molecules are depicted in the **Figures 5-6**

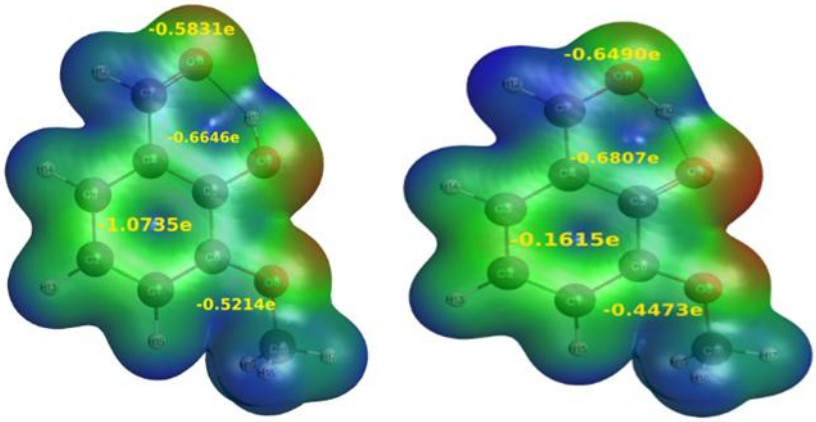

a) **(b)**

Figure-5 : Molecular electrostatic potential with charges on different groups for OVA molecule at (a) S_0 (b) S1 states

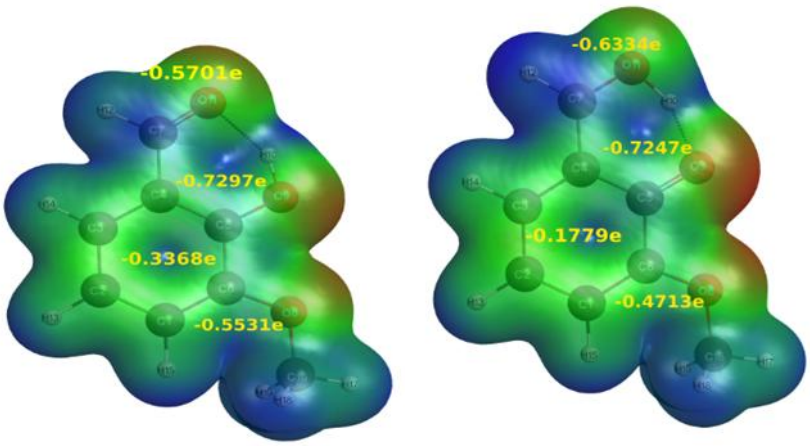

a) **(b)**

Figure-6 : Molecular electrostatic potential with charges on different groups for OVAH molecule at (a) S_0 (b) S1 states

ESIHT process:

In both OVA and OVAH molecules, excited state intra-molecular hydrogen transfer mechanism is observed. In OVA molecule, intra-molecular HB O9-H10·····O11=C7 in S0 state alters as O11-H10·····O9=C5 in the S1 state. In OVAH molecule, intra-molecular HB O9-H10·····O11=C7 in S0 state alters as O11-H10···· ·O9=C5 in the S1 state. i.e., The Hydrogen atom (H10) transfer from the hydroxyl group to benzaldehyde group

at S1 state due to photo-excitation of OVA and OVAH molecules. In OVA molecule, the total charge of hydroxyl group is -0.1583e and that of aldehyde group is 0.1527e in the ground state. But in S1 state, the total charge of hydroxyl group is -0.1735e and that of aldehyde group is 0.2371e. i.e., the charge on H10 increased by 0.0010e and that on O11 increased by -0.0659e due to photo-excitation of OVA molecule. In OVAH molecule, the total charge of hydroxyl group is -0.1055e and that of aldehyde group is 0.2333e in the ground state. But in S1 state, the total charge of hydroxyl group is -0.1536e and that of aldehyde group is 0.2363e. i.e., the charge on H10 increased by 0.0531e and that on O11 increased by -0.0603e due to photo-excitation of OVAH molecule.

IV. Conclusion

In the present work, the structural geometrical parameters, Molecular orbitals and molecular electrostatic potentials of OVA and OVAH molecules have been studied using DFT / TDDFT method with B3LYP/ cc-pVDZ basis set. The stability of both molecules arising from hyper-conjugative interaction and charge delocalization has been analysed using NBO analysis. The molecular electrostatic potential of OVA and OVAH molecules showed suitable regions to attack for electrophilic and nucleophilic substances. The HOMO and LUMO analysis is used to determine the charge transfer within the molecules and the HOMO–LUMO energy gap shows the chemical activity of the molecules. It is observed that, the higher value of HOMO and LUMO energy gap in OVAH molecule showed that the molecule has less chemical reactivity and polarizability. Electrophilicity index(ω) informs about the binding ability of OVA and OVAH molecules with biomolecules. The lower value of electrophilicity index of OVAH molecule showed that it has less binding capacity. While, the higher value of chemical hardness(η) with low negative value of chemical potential(μ) means that the OVAH molecule is a hard molecule with less polarizability. The ESIHT study on OVA and OVAH molecules contributes to the ongoing research on the biological and chemical activity of the molecules.

References

[1]. Chuang M, Ying S. Reconsideration On Hydrogen Bond Strengthening Or Cleavage Of Photoexcited Coumarin 102 In Aqueous Solvent: A DFT/TDDFT Study. Journal Of Computational Chemistry. 2011;32(14): 3058-3061.

[2]. Ramegowda M, Change In Energy Of Hydrogen Bonds Upon Excitation Of 6-Aminocoumarin: TDDFT/EFP1 Study. New J. Chem. 201;37(9): 2648-2653.

[3]. Ramegowda M, A TDDFT/EFP1 Study On Hydrogen Bonding Dynamics Of Coumarin 151 In Water. Spectrochimica Acta Part-A: Molecular And Biomolecular Spectroscopy. 2015;137: 99-104.

[4]. Mingzhen Z, Baiping Ren, Et Al. A DFT/TDDFT Study On The Excited-State Hydrogen Bonding Dynamics Of 6-Aminocoumarin In Water Solution. Spectrochimica Acta Part-A: Molecular And Biomolecular Spectroscopy. 2013; 101:191-195.

[5]. Ramegowda M, Ranjitha KN, Et Al. Exploring Excited State Properties Of 7-Hydroxy And 7-Methoxy 4-Methycoumarin: A Combined Time-Dependent Density Functional Theory/Effective Fragment Potential Study. New Journal Of Chemistry. 2016; 40: 2211-2219.

[6]. Gordon MS, Freitag MA, Et Al. The Effective Fragment Potential Method: A QM-Based MM Approach To Modeling Environmental Effects In Chemistry. The Journal Of Physical Chemistry A. 2001; 105(2): 293–307.

[7]. Ramu YL, Jagadeesha K, Et Al. Microsolvation, Hydrogen Bond Dynamics And Excited State Hydrogen Atom Transfer Mechanism Of 2′,4′-Dihydroxychalcone. Chemical Physics Letters.2020; 739:137030.

[8]. Sardari S, Mori Y, Horita K, Et Al., Synthesis And Antifungal Activity Of Coumarins And Angular Furanocoumarins. Bioorg. Med. Chem. 1999; 7(9): 1933-1940.

[9]. Savarese M, Netti PA, Adamo C, Et Al. Exploring The Metric Of Excited State Proton Transfer Reactions. The Journal Of Physical Chemistry B. 2013; 117(50): 16165–16173.

[10]. Jagadeesha K, Ramu YL, Ramegowda M And Lokanath NK, Excited State Hydrogen Atom Transfer In Micro-Solvated Dicoumarol: A TDDFT/EFP1 Study. Spectrochim. Acta A Mol. Biomol. Spectrosc.2019; 208: 325-330.

[11]. Han KL, Zhao GJ, Hydrogen Bonding Transfer In The Excited State, John Wiley & Sons Ltd.: Newyork. 2011.

[12]. Yi JJ, Wang ZY, Bai HN, Et Al. Optimization Of Purification, Identification And Evaluation Of The In Vitro Antitumor Activity Of Polyphenols From Pinus Koraiensis Pinecones. Molecules. 2015; 20:10450-10467.

[13]. Barbe JC, Bertrand A. Quantitative Analysis Of Volatile Compounds Stemming From Oak Wood, Applications To The Aging Of Wines. Journal Des Sciences Et Techniques De La Tonnellerie. 1996; 2: 83-88.

[14]. Esmaeili A. Biological Activities And Chemical Composition Of The Stems And Roots Of Helichrysum Oligocephalum DC Grown In Iran. Pak. J. Pharm. Sci. 2013; 26: 599-604.

[15]. Zeid AHA, Sleem, AA. "Natural And Stress Constituents From Spinacia Oleracea L. Leaves And Their Biological Activities". Bulletin Of The Faculty Of Pharmacy. 2002; 40 (2): 153–167.

[16]. De A, Ray HP, Jain P, Et Al. Synthesis, Characterization, Molecular Docking And DNA Cleavage Study Of Transition Metal Complexes Of O-Vanillin And Glycine Derived Schiff Base Ligand. J. Mol. Struct.2020; 1199:126901.

[17]. Jong HK, Kathleen LC, Noreen M, Et Al. Antifungal Activity Of Redox-Active Benzaldehydes That Target Cellular Antioxidation. Annals Of Clinical Microbiology And Antimicrobials. 2011; 10, 23.

[18]. Marton A, Kolozsi C, Tubak V, Krisztina B. Vanillin Analogues O-Vanillin And 2,4,6-Trihydroxybenzaldehyde Inhibit Nfkb Activation And Suppress Growth Of A375 Human Melanoma. Anticancer Research. 2016; 36: 5743-5750.

[19]. Husseinzadeh N, Davenport SM. Role Of Toll-Like Receptors In Cervical, Endometrial And Ovarian Cancers: A Review. Gynecol. Oncol. 2014; 135: 359–363.

[20]. Marton A, Kusz E, Kolozsi C, Et Al. Vanillin Analogues O-Vanillin And 2,4,6-Trihydroxybenzaldehyde Inhibit Nfkb Activation And Suppress Growth Of A375 Human Melanoma. Anticancer Res. 2016; 36: 5743–5750.

[21]. Lirdprapamongkol K, Kramb JP, Suthiphongchai T, Et Al. Vanillin Suppresses Metastatic Potential Of Human Cancer Cells Through PI3K Inhibition And Decreases Angiogenesis In Vivo. J. Agric. Food Chem. 2009; 57 :3055–3063.

[22]. Santosh Kumar S, Priyadarsini KI, Sainis KB. Free Radical Scavenging Activity Of Vanillin And O-Vanillin Using 1,1-Diphenyl-2-Picrylhydrazyl (DPPH) Radical. Redox Report-Communications In Free Radical Research. 2013; 7:1: 35-40.
[23]. Hanwell MD, Curtis DE, Lonie DC, Et Al. Avogadro: An Advanced Semantic Chemical Editor, Visualization, And Analysis Platform. J. Cheminform. 2012; 4(1) :17.
[24]. Halgren TA, MMFF VI. MMFF94s Option For Energy Minimization Studies. J. Comput. Chem. 1999; 20(7) : 720 -729.
[25]. Glendening ED, Badenhoop JK, Reed AE, Et Al. NBO 6.0. Theoretical Chemistry Institute, University Of Wisconsin, Madison, WI. 2013.
[26]. Schmidt MW, Baldridge KK, Boatz JA, Et Al. General Atomic And Molecular Electronic Structure System. J. Comput. Chem. 1993; 14(11) :1347-1363.
[27]. Gordon MS, Schmidt MW. Advances In Electronic Structure Theory: GAMESS A Decade Later, In: Theory Applications Of Computational Chemistry, The First Forty Years, Elsevier, Amsterdam. 2005;1167-1189.
[28]. Parr RG, Yang WM. International Academy Of Quantum Molecular Science. Springer. 1980 ; 3: 5-15.
[29]. Kim K, Jordan KD, Comparison Of Density Functional And MP2 Calculations On The Water Monomer And Dimer. J. Phys. Chem.1994; 98(40): 10089-10094.
[30]. Stephens PJ, Devlin FJ, Chabalowski CF, Frisch MJ, Ab Initio Calculation Of Vibrational Circular Dichroism Spectra Using Accurate Post-Self-Consistent-Field Force Fields: Trans-2,3-Dideuteriooxirane. J. Phys. Chem.1994; 97(23): 6107–6110.
[31]. Cundari TR, Stevens WJ. Effective Core Potential Methods For The Lanthanides. J. Chem. Phys. 1993; 98: 5555-5565.
[32]. Hay PJ, Wadt WR. Ab Initio Effective Core Potentials For Molecular Calculations. Potentials For K To Au Including The Outermost Core Orbitals. The Journal Of Chemical Physics.1985; 82: 299-310.
[33]. Tokura S, Sato T, Tsuneda T, Nakajima T, Hirao K, A Dual-Level State-Specific Time-Dependent Density-Functional Theory. J. Comput. Chem. 2008; 29(8):, 1187-97.
[34]. Chiba M, Tsuneda T, Hirao K, Excited State Geometry Optimizations By Analytical Energy Gradient Of Long-Range Corrected Time-Dependent Density Functional Theory. J. Chem. Phys. 2006; 124 :144106.
[35]. Becke AD, Density-Functional Thermochemistry. III. The Role Of Exact Exchange J. Chem. Phys.1993; 98 :5648-5652.
[36]. Becke AD, Density-Functional Exchange-Energy Approximation With Correct Asymptotic Behavior. Phys. Rev. A Gen. Phys.1988; 38, 3098.
[37]. Dunning TH Jr. Gaussian Basis Sets For Use In Correlated Molecular Calculations. I. The Atoms Boron Through Neon And Hydrogen. J. Chem. Phys. 1989; 90 :1007-1023.
[38]. Furche F, Ahlrichs R. Adiabatic Time-Dependent Density Functional Methods For Excited State Properties. The Journal Of Chemical Physics. 2002;117(16) :7433-7447 .
[39]. Li H, Pomelli CS, Jensen JH. Continuum Solvation Of Large Molecules Described By QM/MM: A Semi-Iterative Implementation Of The PCM/EFP Interface. Theor. Chem. Acc. 2003; 109 :71-84.
[40]. Perdew J, Ernzerhof M, Burke K. Rationale For Mixing Exact Exchange With Density Functional Approximations. The Journal Of Chemical Physics. 1996; 105: 9982.
[41]. Bode BM, Gordon MS. Macmolplt: A Graphical User Interface For GAMESS. Journal Of Molecular Graphics And Modelling. 1998 ; 16 (3): 133-8.